Available online at www.sciencedirect.com
SCIENCE DIRECT
Polymer 46 (2005) 5608–5614
polymer
www.elsevier.com/locate/polymer

Morphology and micromechanical behaviour of ethylene cycloolefin copolymers (COC)

V. Seydewitz[a,*], M. Krumova[b], G.H. Michler[a,b], J.Y. Park[c], S.C. Kim[c]

[a]*Institute of Polymeric Materials at the Martin Luther University Halle-Wittenberg, Geusaer Straße, D-06217 Merseburg, Germany*
[b]*Institute of Materials Science, Martin Luther University Halle-Wittenberg, D-06099 Halle (Saale), Germany*
[c]*Department of Chemical and Biomolecular Engineering, Korea Advanced Institute of Science and Technology (KAIST), Kusungdong, Yusongku, Taejon 305-701, South Korea*

Received 27 August 2004; received in revised form 15 December 2004; accepted 2 May 2005
Available online 3 June 2005

Abstract

Cyclic olefin copolymers (COC) of ethylene and different types of cyclic monomers were investigated in detail. In particular, the influence of the type and the content of cyclic monomers on the micromechanical deformation behaviour was studied using electron microscopy. Several deformation modes as fibrillated crazes, homogeneous deformation zones, shear-bands, and occasionally a combination of some of these deformation structures were observed in these materials. The different deformation modes are correlated with the mechanical properties. A tendency to an increase in brittleness with increasing cyclic monomer content was observed. COC with larger side chains in the cyclic monomer show a more ductile behaviour with the corresponding deformation structures than COC with norbornene.

Keywords: Polymer materials; Micromechanical behaviour; Electron microscopy

1. Introduction

Cyclic olefin copolymers are materials which attained economic relevance only in the last few years, although first developments range back to over 40 years. The beginnings were in Dupont in the USA followed by Montecatini in Italy (with support of Nobel prize winner Guilio Natta), by the 'Leuna Werke' in Eastern Germany and by Mitsui in Japan. Recent progress in metallocene catalysts enabled the industrial production of cyclic olefin copolymers of large structural and performance variety [1].

Cyclic olefin copolymers (COC) form a new class of copolymers with excellent optical, thermal and permeation properties. The copolymerization of olefins with a cyclic monomer leads to predominantly amorphous materials with relatively high glass transition temperatures, exhibiting numerous useful physical qualities, such as high optical transparency, low birefringence, low moisture absorption etc. [2]. These properties are very interesting for application in medicine and optics, especially for laser-optical devices like CDs, DVDs and optical lenses. Their high temperature resistance (compared with polycarbonate for example) combined with low dissipating and dielectric loss factors makes COC's suitable also for microelectronic applications.

The properties of the COC depend strongly on the comonomer combination. At least one comonomer is a cycloolefin of norbornene type, the other belongs to the group of the 1-olefines [3]. Beside traditional norbornene, also substituted norbornens or its higher homologes and their substituted variations can be used.

The majority of the published works deals predominantly with copolymers between ethylene and traditional norbornene. The papers correlate thermal and thermomechanical properties with monomer content and microstructure [4–8]. Few reports are devoted to mechanical investigations [9,10]. Macroscopically the COC's break in a brittle manner, nevertheless different local micromechanical processes are possible, which are very similar to the craze-like deformation zones in styrene–acrylonitrile-copolymers (SAN) [11]. In brittle materials fibrillated crazes, homogeneous deformation zones, shear-bands and occasionally a

* Corresponding author. Tel.: +49 3461 462764; fax: +49 3461 462535.
E-mail address: volker.seydewitz@iw.uni-halle.de (V. Seydewitz).

0032-3861/$ - see front matter © 2005 Elsevier Ltd. All rights reserved.
doi:10.1016/j.polymer.2005.05.029

Table 1
Cyclic monomers in the samples investigated

A-series	B1	B2	B3	C2,C3	D-series
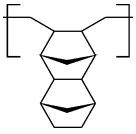	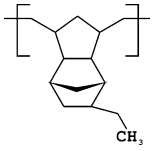	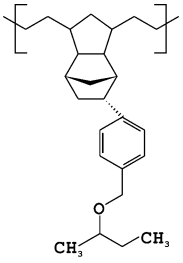	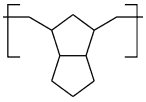	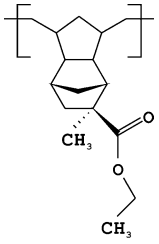	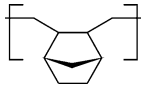

Trivial: norbomene

combination of some of these deformation structures are frequently observed [11,12].

The aim of the present study is to investigate the micromechanical behaviour of COC's depending on type of the cyclic monomer and its molecular content using methods of electron microscopy and to contribute to the understanding of their macroscopic mechanical performance.

2. Experiment

2.1. Materials

The materials studied were commercial grades of cyclic olefin copolymers (designated further as COC) from different producers: the Mitsui Chemicals Inc. Tokyo (Japan), Japan Synthetic Rubber Co. Mie (Japan), Zeon Chemicals Co. Okayama (Japan) and Ticona GmbH Oberhausen (Germany). All examined specimens contain ethylene as one monomer. The differences consist on one hand in the type of the cyclic monomer and on the other hand in its volume fraction. The chemical structures of the cyclic monomers are shown in Table 1. Series A and D contain different amounts of the same cyclic comonomer. Table 2 summarizes the content of cyclic monomer and the corresponding glass transition temperatures (T_g) in the series. The mechanical properties of the samples investigated in this study are listed in Table 3.

2.2. Sample preparation and methods

Morphological investigations of the specimens were performed by conventional transmission electron microscopy (TEM) on ultrathin sections of the materials. First, blocks of the samples trimmed to the shape of a pyramid, were stained with RuO_4 vapor for contrast enhancement. After that, ultrathin sections of 70 nm were cut using a diamond knife equipped Ultracut E, Leica ultramicrotome. For the observations an JEOL transmission electron microscope JEM 2010 operated at 200 kV acceleration voltage was used.

The micromechanical behavior was studied on 5 to maximum 12 specimens of the same COC type in a high voltage electron microscope (HVEM JEOL 1000) of the Max Planck Institute of Microstructure Physics in Halle operated at 1000 kV. Semithin sections of 1 μm, about 4 mm long and 0.5 mm wide, were cut from the bulk material using an ultramicrotome RMC MT-7. Each section was fixed between two adhesive tapes with a central hole of 1 mm in diameter. After transferring this sandwich into a special miniature tensile-desk, the adhesive tapes were cut in transverse direction in the areas adjacent to the central hole. The self-supported semithin sections were deformed either outside the HVEM under light microscope control or 'in situ' inside the HVEM. This technique is described in detail in Ref. [14].

3. Results

3.1. Morphological investigations of COC-samples

COC are supposed to be amorphous. Nevertheless, an attempt was made to detect local microstructures in TEM. Applying the standard RuO_4 staining no more than local density fluctuations in the majority of the samples investigated was registered, as shown for example in Fig. 1 for the sample D2.

Theoretical considerations predict however some

Table 2
T_g and cyclic monomer content ([13])

	A2	A5	B1	B2	B3	C2	C3	D2	D3	D5
Cont. mol%	21.4	32.2	52	50.5	53.7	51	51.6	57.7	61.5	65.9
T_g (°C)	80	145	138	139	105	171	176	149	162	177

Table 3
Mechanical properties

Properties	A2	A5	B1	B2	B3	C2	C3	D2	D3	D5
Tensile strength[a] (MPa)	60	60	60	72	53	75	75	66	66	66
Elongation[a] (%)	30	3	40	10	60	15	15	4	4	4
Flexural modulus[a] (MPa)	2700	3200	2100	2500	2100	3000	3000	–	–	–
Notched Izod impact strength[b] (Jm)	21	12	23	20	19	8	7	14	17	12

[a] Data obtained from suppliers.
[b] Data measured by Izod impact tester.

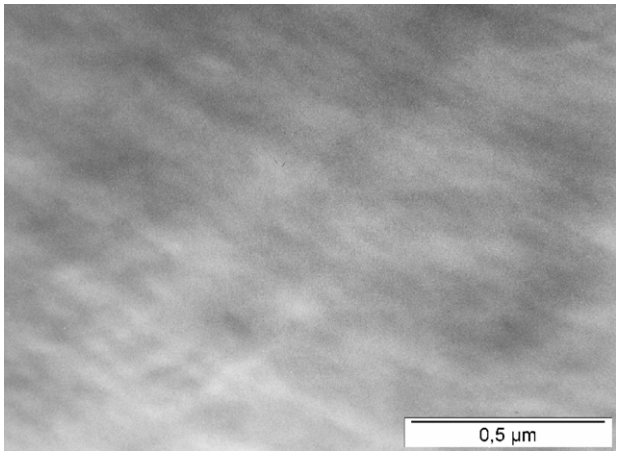

Fig. 1. TEM-micrograph of sample D2: no significant contrast occurs. 200 keV, RuO_4-staining.

crystallisation in copolymers with alternating ethylene and norbornene sequences, which was supported by DSC measurements [3]. X-ray diffraction studies have found reflections, located at different 2θ angles [15,16], but the interpretations are still ambiguous and controversial. To our knowledge no direct visualisation of semicrystalline structure in COC's using electron microscopy has yet succeeded.

After rather heavy staining procedure we observed occasionally lamella-like structures also in COC's comprising ramification of the norbornene comonomer. The reason for this phenomenon is not clear yet.

3.2. Micromechanical deformation structure of COC

The samples under investigation are characterised by different molecular structures and show different glass transition temperatures (Tables 1 and 2). Therefore, differences in their micromechanical behaviour can be expected.

Several deformation modes are generally known for brittle and semi ductile polymeric systems: fibrillated crazes, homogeneous deformation zones, shear bands, and occasionally a combination of two or more of these deformation structures. The different micromechanical deformation structures are sketched in Fig. 2. These different micromechanical deformation modes reveal a correlation with the mechanical performance as indicated in the figure. Interestingly, one can find almost all of them in the present systems.

Figs. 3–12 show the deformation structures of the investigated specimens. In specimen A2 homogenous deformation zones with crazes inside (called 'intrinsic crazes') were observed (Fig. 3). In sample A5 also homogenous deformation occurs. Furthermore, numerous single fibrillated intrinsic crazes and additional enlarged voids can be recognised (Fig. 4). Also single fibrillated crazes are formed outside of the large homogenous deformation zone (Figs. 4 and 5).

Fig. 6 demonstrates the appearance of multiple crazing and shear deformation (shear bands under 45° to the deformation direction) in specimen B2. This specimen can deform also in form of homogenous deformation zones with intrinsic crazes and voids in the crazes (Fig. 7). Most of the crazes show void formation in the middle. Similar

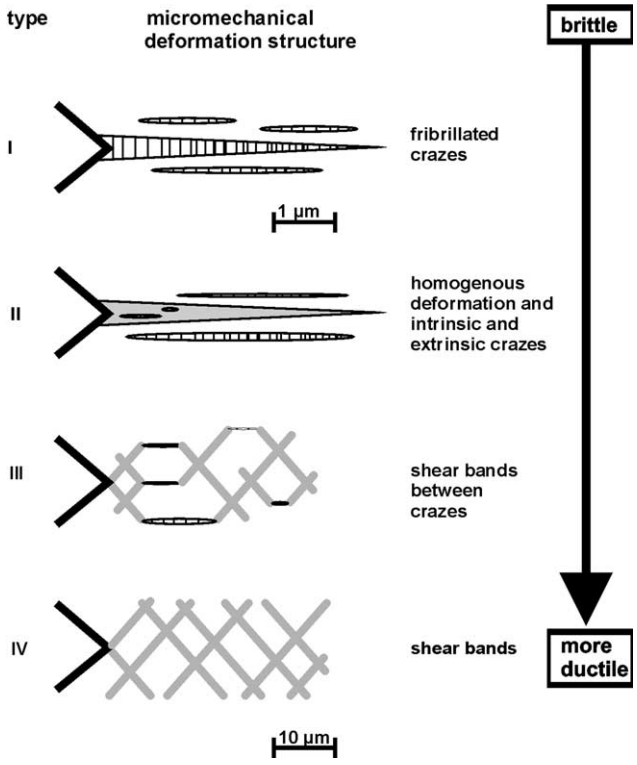

Fig. 2. Changes in the micromechanical deformation structures with transition from brittle to ductile behaviour, deformation direction perpendicular and propagation of the deformation zones from left (starting at a notch) to right (after [11]).

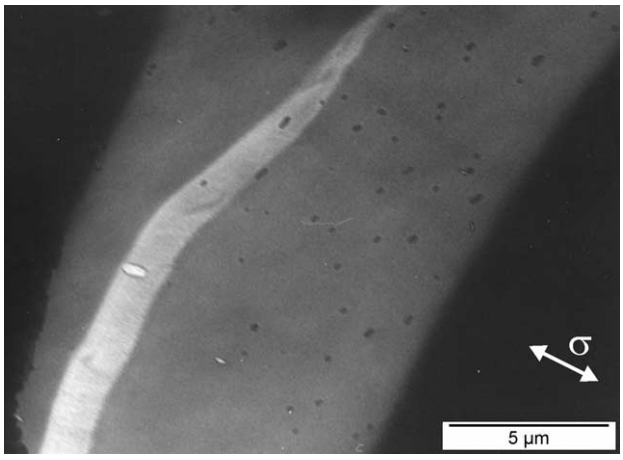

Fig. 3. Micromechanical deformation structures in sample A2: homogeneous deformation zones with intrinsic crazes occur. HVEM-micrograph, deformation direction perpendicular to 'bright' structure (see arrow).

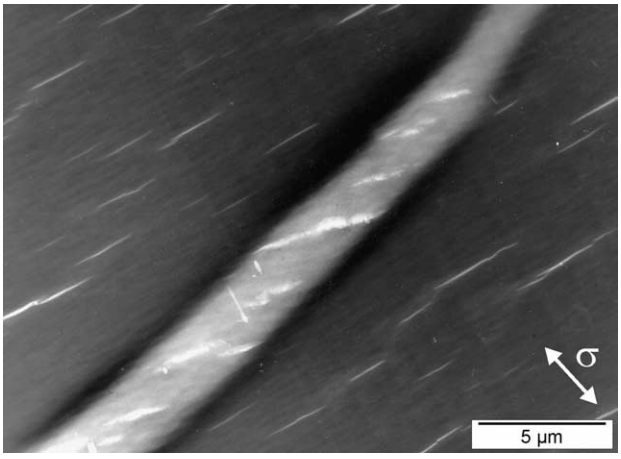

Fig. 4. Micromechanical deformation structures in sample A5: multiple crazes and homogeneous deformation with intrinsic crazes and voids occur. HVEM-micrograph.

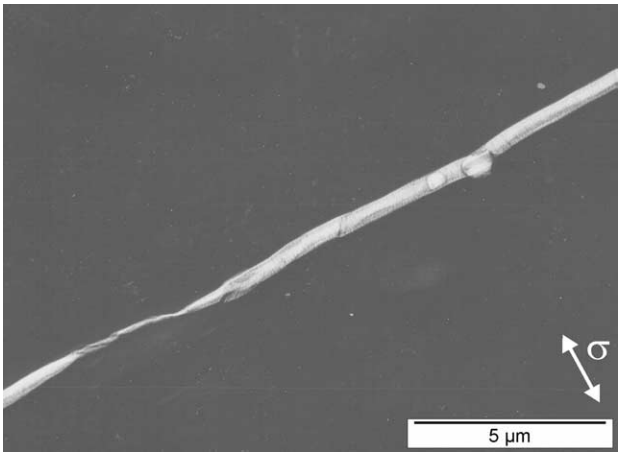

Fig. 5. Micromechanical deformation structures in sample A5: single fibrillated craze. HVEM-micrograph.

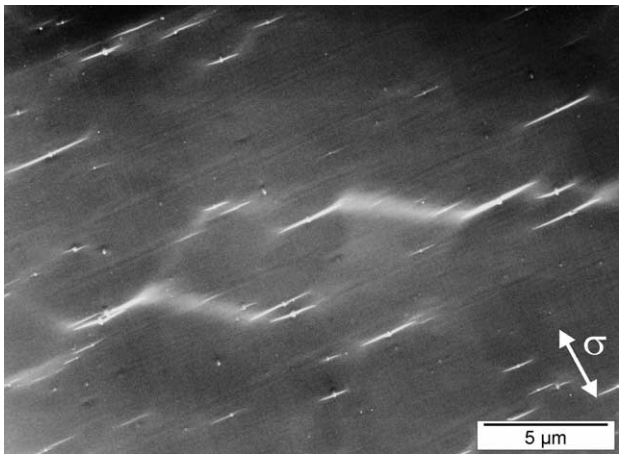

Fig. 6. Micromechanical deformation structures in sample B2: shear deformation and multiple crazes can be seen. HVEM-micrograph.

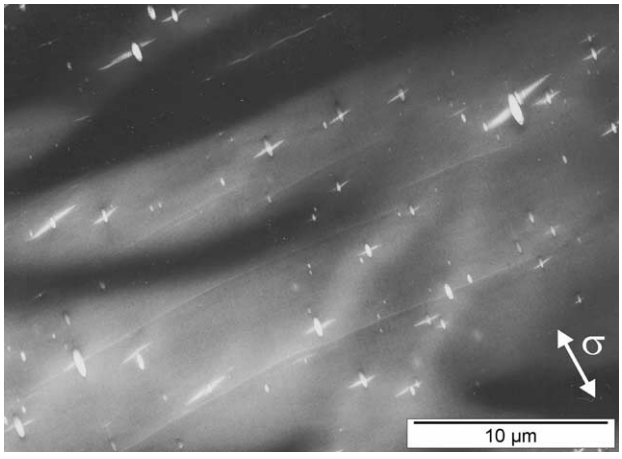

Fig. 7. Micromechanical deformation structures in sample B2: homogeneous deformation zones with intrinsic crazes and voids in crazes are visible in this specimen. HVEM-micrograph.

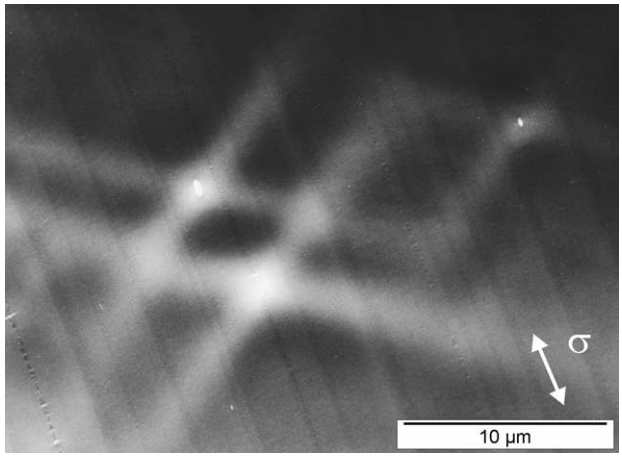

Fig. 8. Micromechanical deformation structures in sample C2: shear band deformation (with shear bands at an angle of 45° to the principal stress direction) are observable. HVEM-micrograph.

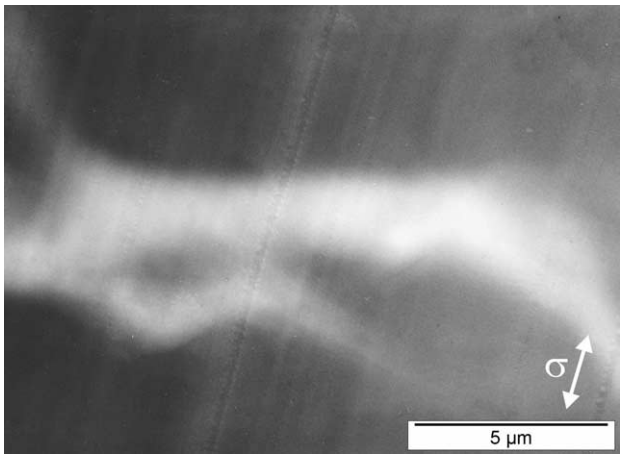

Fig. 9. Micromechanical deformation structures in sample C3: shear deformation (bands and zones). HVEM-micrograph.

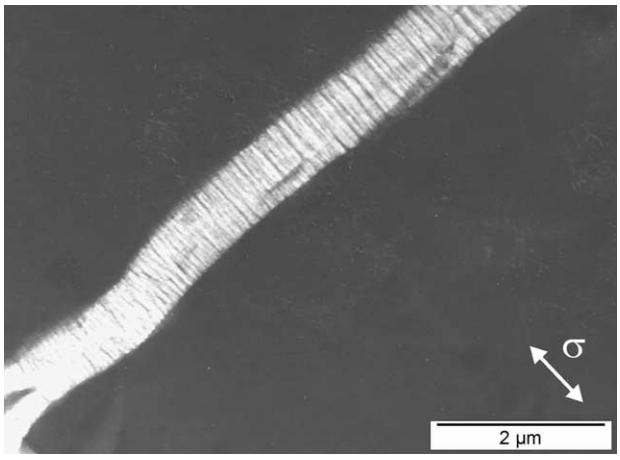

Fig. 11. Micromechanical deformation structures in sample D3: single fibrillated crazes are visible. HVEM-micrograph.

deformation structures were observed in specimen B3 (results not presented here).

Shear band deformation occurs in C2 (Fig. 8), while diffuse homogeneous deformation zones and shear-bands are visible in sample C3 (Fig. 9).

The D-series shows the whole variety of crazes: fibrillated only at the border to the undeformed material (sample D2, Fig. 10), completely fibrillated (sample D3, Fig. 11), unfibrillated (narrow homogenous) crazes (sample D5, Fig. 12).

These results, together with additional details about the deformation structures are summarised in Table 4.

4. Discussion

The micromechanical deformation structures in the investigated COC materials are similar to the structures observed in other brittlelike amorphous polymers, as polystyrene (PS), styrene–acrylonitrile-copolymer (SAN), polyvinylchloride (PVC) etc. [11]. The type of the microdeformation structures correlates with the mechanical performance of the materials. Fig. 2 shows their changes with increasing ductility: starting from fibrillated crazes (type I, characteristic for the brittle PS), through homogeneous crazes or homogeneous deformation zones (type II), shear bands (type III) until multiple shearing (type IV), characteristic for elevated ductility. Some of these structures can also appear in parallel.

From the investigation of the COC, it can be stated that all the specimens of series A, B and C (i.e. series with more side chained cyclic monomers or without norbornene) deform at least partially via shear deformation or homogenous deformation. In other words, these samples show a more ductile deformation behaviour compared to the copolymers containing traditional norbornene. This trend is in a good agreement with the macroscopic measurements of elongation at break ε (Table 3) where all specimen except A5 and the D-series show $\varepsilon > 10\%$.

The micromechanical deformation behaviour of the

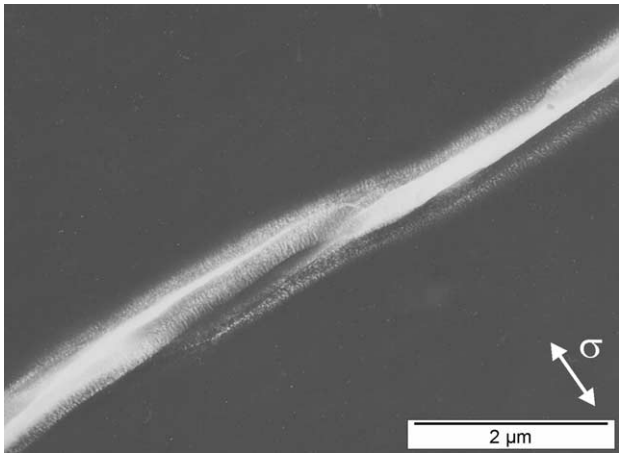

Fig. 10. Micromechanical deformation structures in sample D2: fibrillated crazes with 'bright' middle zones dominate in this specimen. HVEM-micrograph.

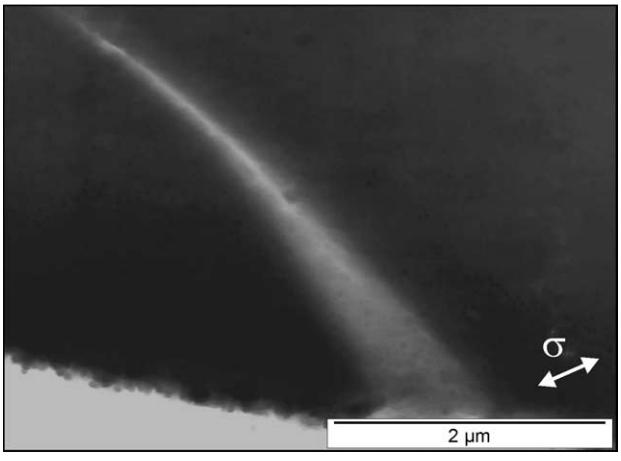

Fig. 12. Micromechanical deformation structures in sample D5: single unfibrillated crazes are visible. HVEM-micrograph.

Table 4
Deformation behaviour of the COC

Sample	A2	A5	B1	B2	B3	C2	C3	D2	D3	D5
Micro-mechanical deformation structure	Homogenous deformation zones with 'intrinsic crazes'	Homogenous deformation zones with intrinsic razes'	Homogenous deformation with void formation	Homogeneous deformation with inner shear bands and crazes with voids	Homogenous deformation zones with intrinsic crazes	Shear deformation with voids	Shear deformation	Long crazes 8–25 μm fibrillated at the boundaries	Narrow fibrillated crazes	Homogeneous crazes
		Multiple crazing extrinsic fibrillated crazes		Regions with high number of small crazes	Shear deformation between crazes					
Craze size	300–500 nm	75–100 nm		200–500 nm	200–500 nm			200–500 nm	750 nm	
Thickness of craze fibrils	~30 nm	50 nm		<50 nm	<50 nm			<50 nm	50–70 nm	
Deformation type (Fig. 2)	II	I,II	II	I,II,III	I,II,III	IV	IV	I,II	I	I,II
Deformed undeformed volume ratio	<5%	<5%	<5%	<10%	<5%	<15%	<15%	<10%	<5%	<5%

samples of series A and D can be followed as a function of the cyclic monomer content. As described above, the sample A2 (Fig. 2) with a relatively low content of cyclic monomer (Table 2) deforms via formation of homogeneous deformation zones with intrinsic crazing. In sample A5 with a 10% higher cyclic monomer content, homogenous deformation zones occur in addition with multiple crazing and more void formation in the intrinsic crazes (Fig. 4). Also 'extrinsic' fibrillated crazes (single crazes) with voids can be found (Fig. 5). These results indicate that the ductility of the samples decreases with increasing cyclic monomer content. The elongation at break and the notched Izod impact strength show the same behaviour (Table 3).

In the series with different norbornene fraction (series D) the sample D2 with the lowest norbornene content is a typical example for the formation of crazes with voiding and fibrillation at the craze boundaries and a homogenous deformation in the middle of the craze (Fig. 10), similar to the fibrillated crazes with a bright mid-rib in SAN polymers. With increasing norbornene fraction, both fibrillated (such as in D3, Fig. 11) and unfibrillated (such as in D5, Fig. 12) crazes arise. In these samples with a relatively high norbornene content extended homogenous deformation zones or shear bands do not appear. Such 'ductile' deformation zones cannot be expected in the samples of the D series since the sample with the lowest norbornene content (D2) already exhibits deformation structures typical for brittle materials. This can be supported by the low elongation at break ($\varepsilon = 4\%$) of all samples of D-series.

These observations indicate that the ductility of the samples decreases with increasing cyclic monomer content. The explanation can be found in the relatively rigid atom arrangement of the cyclic monomers, which obstructs the mobility of the whole copolymer macromolecule. The results are supported also by the estimation of the ratio between the deformed and undeformed volume, presented in Table 4. This ratio can be estimated from electron micrographs of deformed semithin sections just before they break. Since the specimen for electron microscopic investigations are relatively thin, the estimation of this ratio can be reduced in first approximation to the quotient of a part of deformed areas (crazes, deformation zones, shear bands,…) to the undeformed area. Now it has been considered that the volume content of the plastically deformed polymeric material in the deformation zones is in the order of 25–50% (compare Refs. [11,12] for crazes). Therefore, the volume ratio will be roughly the half of the measured area ratio. This estimation is more sensitive to reveal the influence of the molecular structure of the investigated COC on the micromechanical deformation process than macroscopic measurements.

Another trend can be found comparing the deformation behaviour of the COC-samples with the different cyclic monomers. The samples B2, C2 and C3, i.e. the samples comprising longer side chains in the cyclic monomer show deformation structures corresponding to a higher ductility

than the D-series (Table 4). Especially, samples C2 and C3 with a pronounced shear band deformation show a larger stretched volume (largest ratio of deformed/undeformed volume). Some discrepancy can be found with the macroscopic deformation values (elongation at break, notched Izod impact strength). It can be supposed that the influence of the complicated structure of the cyclic monomer on the deformation behaviour of these samples is better expressed on microscopic scale, than in the averaged macroscopic deformation values, which are also influenced by sample preparation defects, such as micro-cracks, scratches, etc.

Acknowledgements

This study forms part of a project of the IUPAC Working Party IV.2.1. 'Structure and Properties of Commercial Polymers'. We gratefully acknowledge Mrs E. Kühnberger and Mr J. Laatsch for performing some electron microscopic investigations. The authors are indebted to the Ministry of Culture of Saxony-Anhalt for financial support.

References

[1] Thayer AM. Chem Eng News 1995;11.
[2] Khanarian G. Opt Eng 2001;40:1024–9.
[3] Cherdron H, Brekner MJ, Osan F. Angew Makromol Chem 1994;223:121–33.
[4] Forsyth J, Scrivani T, Benavente R, Marestin C, Rerena JM. J Appl Polym Sci 2001;82(9):2159–65.
[5] Forsyth J, Perena JM, Benavente R, Pérez E, Tritto I, Boggioni L, et al. Macromol Chem Phys 2001;202:614–20.
[6] Scrivani T, Benavente R, Pérez E, Perena JM. Macromol Chem Phys 2001;202(12):2547–53.
[7] Shih HH, Shiao PL, Hsu HC, Liu HJ, Huang CJ, Tsai CC. J Appl Polym Sci 2002;86(14):3695–701.
[8] Ruchatz D, Fink G. Macromolecules 1998;31:4674–80.
[9] Zamfirova G, Misheva M, Pérez E, Benavente R, Cerrada ML, Djoulov N, et al. Polym J 2002;34(11):779–85.
[10] Djourelov N, Misheva M, Zamfirova G, Benavente R, Pérez E, Perena JM. Macromol Chem Phys 2003;204(12):1531–8.
[11] Michler GH. Kunststoff-Mikromechanik. München: Carl Hanser Verlag; 1992 chapter 7, p. 140–84.
[12] Crazing in polymers—vol. 1. In: Kausch HH, editor. Advances in polymer science, vols. 52/53. Berlin: Springer-Verlag; 1983. Crazing in polymers—vol. 2. In: Kausch HH, editor. Advances in polymer science, vols. 91/92. Berlin: Springer-Verlag; 1990.
[13] Shin JY, Park JY, Liu C, He J, Kim SC. Pure Appl Chem 2005;77(5):801–14.
[14] Michler GH, Lebek W. Ultramikrotomie in der Materialforschung. München: Carl Hanser Verlag; 2004 chapter 7.2, p. 149–59.
[15] Rische T, Waddon AJ, Dickinson LC, MacKnight WJ. Macromolecules 1998;31:1871–4.
[16] Haselwander TFA, Heitz W, Krügel SA, Wendorff JH. Macromol Chem Phys 1996;197(10):3435–54.